NONLINEAR EVOLUTION OF A TURBULENT SPECTRUM OF OUTWARDLY PROPAGATING ALFVÉN WAVES IN SOLAR AND STELLAR CORONAE

Andrea Verdini[(1)], Marco Velli[(1)], and Sean Oughton[(2)]

[(1)]*Dipartimento di Astronomia e Scienza dello Spazio, Firenze, Italy*
[(2)]*Department of Mathematics, University of Waikato, Private Bag 3105, Hamilton, New Zeland*

ABSTRACT

We investigate the non-linear evolution of Alfvén waves in a stratified corona with wind, from the base out to the Alfvénic point, where the wind speed equals the velocity of the waves. We consider both an isothermal corona, with spherically expanding flux tubes, and the more realistic case of a corona and wind where the flux-tube expansion is supraspherical and the temperature peaks at about $3\ R_\odot$ and then falls off. Nonlinear interactions, triggered by wave reflection due to the atmospheric gradients, are assumed to occur mainly in directions perpendicular to the mean magnetic field. The nonlinear coupling between waves propagating in opposite directions is modeled by a phenomenological term, containing an integral turbulent length scale. Low frequency waves, which suffer the strongest reflection, drive dissipation for waves across the whole spectrum; lower coronal temperatures, by increasing density gradients and therefore reflection, also enhance the dissipation rate. We find also that for typical coronal gradients, the power-law index of a wave-spectrum does not change much from the coronal base to the Alfvén point.

1. INTRODUCTION

One of the most promising mechanisms for heating the open solar corona is the development of MHD turbulence driven by the reflection of Alfvén waves.
The presence of MHD waves inside the solar corona has been proved indirectly by measurements involving Faraday rotation at distances of $\sim 8R_\odot$ from the sun's surface (Hollweg et al., 1982), while much farther away "in situ" measurement of magnetic and velocity field fluctuations from Helios and Ulysses have revealed a broad developed spectrum for frequencies ranging from $10^{-4}\ Hz$ to $10^{-2}\ Hz$ (for the fast component of the solar wind). Typically, a strong correlation between magnetic field and velocity fluctuations in this distance range persists (Mangeney et al., 1991). At intermediate distances (from 10 to 40 solar radii) ground based radio scintillation measurements using radio sources (Scott et al., 1983) have shown velocity field fluctuations to increase together with bulk flow speed (both around $\sim 200\ km/s$) but data on correlated magnetic field fluctuations are still missing. Moreover, if one assumes the origin of the MHD fluctuations to lie in photospheric motions at the Sun's surface, one would expect some signature in the observations of a frequency corresponding to the characteristic time-scale of the energy injection at that level, while no such signal is observed. One is then tempted to suppose that strong nonlinear interactions are at work from the very beginning and that the original wave spectrum is modified during propagation through the outer atmosphere by the development of a turbulent cascade. In this way the energy is exchanged between modes of different frequencies and transferred toward smaller scales where dissipation becomes efficient.
It is well known that nonlinear terms couple Alfvén waves propagating in opposite directions whereas one expects waves to propagate only outward, as observed in fast solar wind streams.
The inhomogeneities of the ambient medium suggest a solution for this apparent contradiction between unidirectional propagation and developing of nonlinear interaction. Variations of the group velocity of the wave (Alfvén speed gradient) linearly couple the outgoing and ingoing waves producing one from the other and furnishing the background for nonlinear interactions to take place.
Intensive studies of this mechanism have been carried out in terms of the dynamical time scales which enter the governing equation, the anisotropic nature of the problem was handled naturally in the context of an RMHD description which allows one to treat properly non linear terms (Dmitruk et al., 2000, 2002; Dmitruk and Matthaeus, 2003; Oughton et al., 2001, 2004). This kind of approach has led to the understanding of the ordering of the characteristic times which should effectively favor the development of a turbulent cascade in planes perpendicular to the direction of wave propagation (along the magnetic field) and the efficiency of dissipation. Other authors (Heinemann and Olbert, 1981; Leroy, 1980, 1981; Krogulec et al., 1994; Krogulec and Musielak, 1998; Lou and Rosner, 1994; Mangeney et al., 1991; Velli et al., 1991; Velli, 1993; Moore et al., 1991; Similon and Zargham, 1992, but also Dmitruk et al., 2001 for a phenomenological non linear model) have focused their attention on the linear aspect involving wave propagation. As a result three main features have proved to be essential. The first one concerns the geometry of the medium, the second one concerns the extension of the atmosphere whose global stratification determines the transmission of waves at a given frequency, and finally the third aspect involves the presence of a wind which separates the atmosphere into two parts. The Alfvén critical point (the distance from the sun at which the wind speed equals the Alfvén speed) represents a natural separation between an internal region where the wind is slow and affects the propagation of the waves only slightly (at least at high frequencies) and an outer region, beyond the critical point, where the waves are advected by the wind expansion. The aim of this paper is to investigate non-

linear effects on wave propagation and spectra modification once the background medium and the entire (lower) atmosphere are taken into account. Following Dmitruk et al., 2001, we choose a constant transverse dissipative length scale but we introduce frequency coupling to account energy redistribution inside the spectrum.

2. THE MODEL

The equations describing the propagation of Alfvén waves in an inhomogeneous stationary medium can be derived from the MHD equations under the hypotheses of incompressible adiabatic transverse fluctuations. The velocity ($\mathbf{v}$) and magnetic field fluctuations ($\mathbf{b}$) can be combined to form the Elsässer variables $\mathbf{z}^{\pm} = \mathbf{u} \mp sign(\mathbf{B_0})\mathbf{b}/\sqrt{4\pi\rho}$ which describe Alfvén waves propagating outward ($\mathbf{z}^{+}$) or inward ($\mathbf{z}^{-}$). $\mathbf{B_0}$ stands for the average magnetic field and the sign is taken with respect to the outward direction on the field line while ρ represents the mass density (not constant) of the ambient medium. In terms of these variables we can write down the equations for the two fields

$$\frac{\partial \mathbf{z}^{\pm}}{\partial t} + [(\mathbf{U} \pm \mathbf{V_a}) \cdot \boldsymbol{\nabla}]\mathbf{z}^{\pm} + (\mathbf{z}^{\mp} \cdot \boldsymbol{\nabla})(\mathbf{U} \mp \mathbf{V_a}) + \\ + \frac{1}{2}(\mathbf{z}^{-} - \mathbf{z}^{+})[\boldsymbol{\nabla} \cdot \mathbf{V_a} \mp \frac{1}{2}(\boldsymbol{\nabla} \cdot \mathbf{U})] = -(\mathbf{z}^{\mp} \cdot \boldsymbol{\nabla})\mathbf{z}^{\pm} + \\ -\frac{1}{\rho}\boldsymbol{\nabla} p_{tot} \qquad (1)$$

where $\mathbf{U}$ is the mean wind speed and the Alfvén speed is $\mathbf{V_a} = \mathbf{B_0}/\sqrt{4\pi\rho}$, colinearity between magnetic and gravitational field is assumed. On the right hand side we have grouped the nonlinear terms including total (magnetic plus gas) pressure, which in the limit of incompressible fluctuations can be written as combinations of the product $\mathbf{z}^{+} \cdot \mathbf{z}^{-}$. The nonlinear terms which don't average to zero are to be considered part of the background medium equation. In the linear part of the eq.1 we can recognize a propagation term (II) and two terms accounting for reflection due to the variation of the properties of the medium, one isotropic (IV) while the other (III) involves variations along the fluctuations' polarization. One can clearly see how reflection linearly couples the equations for the two counter-propagating waves.

2.1 The background atmospheres

An isothermal atmosphere is completely defined by setting the values for temperature, density and magnetic field intensity at the base together with mass and radius of the central object ($M_\odot$ and $R_\odot$). Nevertheless, with regards to wave propagation, we are only interested in wind speed and Alfvén speed profiles (and their derivatives) which are selected among the solutions imposing the two parameters α, the adimensional scale height, and β, the plasma parameter at the base,

$$\alpha = \frac{GM_\odot}{R_\odot c_s^2} \sim \frac{v_{esc}^2}{c_s^2} \text{ and } \beta = \left(\frac{P}{B^2/8\pi}\right)_0 \sim \frac{c_s^2}{V_{a0}^2}. \quad (2)$$

(c_s is the sound speed, $v_{esc} = \sqrt{2GM_\odot/R_\odot}$ is the escape speed from sun surface). This allows one to solve numerically the implicit equation for the isothermal wind (whose temperature is fixed at the critical point, $r = R/R_\odot$ and A is the flux tube expansion, equal to r^2 for the spherical case),

$$\left(\frac{U^2}{c_s^2} - 1\right)\frac{U'}{U} = \frac{A'}{A} - \frac{\alpha}{r^2} \qquad (3)$$

and then obtain the profile for Alfvén speed,

$$\frac{V_a(r)}{c_s} = \sqrt{\frac{2}{\beta}\frac{U(r)}{U_0}\frac{A_0}{A(r)}} \qquad (4)$$

The values at the base for mass density and magnetic field intensity are related by the Alfvén speed definition ($\rho_0 = B_0^2/4\pi V_{a0}^2$), so one has to impose only one of the two, while their profiles are fixed by flux conservation equations, $\rho = \rho_0 A_0/A(r) \times U_0/U(r)$ and $B = B_0 A_0/A(r)$

We also consider a more realistic Solar case, in which the wind expands super-radially, as from the sun's coronal holes. Streamlines follow a flux tube expansion of the form $A = fr^2$ with f a function which has a maximum close to the coronal base and tends to 1 at large distances (see Kopp & Holzer, 1976, and Munro & Jackson, 1977). The temperature profile fitted to Sun's observations starts at about 8 10^5 K at the coronal base, peaks at about 3 10^6 K at 3 R_s and then falls off with distance as $R^{-0.7}$ (see Casalbuoni et al., 1999). Eq.3 slightly changes, since on the RHS we have to include the temperature variation ($+T'/T$), and the sonic critical point is not determined a priori but it must be found with an iterative procedure. Flux tube expansion modifies the conservation equation for the mass and the magnetic field, hence also the Alfvén and the wind speeds, producing a heavier stratification in the expansion region (enhanced reflection).

2.2 Non-linear interactions

Since the ambient medium is in stationary equilibrium we can Fourier transform with respect to time and identify propagating fluctuation with waves at a given frequency ω. Following Dmitruk et al. (2001) we choose the following model for the nonlinear terms in eq.(1)

$$NL_j = \mathbf{z}^{\pm}(\omega_j)\frac{|\mathbf{Z}^{\mp}(\omega_1, .., \omega_n)|}{L} = \mathbf{z}^{\pm}(\omega_j)\frac{\sqrt{\Sigma_1^n |\mathbf{z}^{\mp}(\omega_i)|^2}}{L} \qquad (5)$$

where L represents an integral turbulent dissipation length and $\mathbf{Z}^{\pm}$ stands for the total amplitude of the Elsässer field at the point r, (hence including, for a given frequency, coupling to all others) .
Alternatively, the coupling can be considered local in frequency so that only waves of the same frequency interact nonlinearly. In this case the dissipation rate is independent of the way the energy is distributed and is determined essentially by the local frequency-dependent reflection rate.

In the first case, the energy distribution over the spectral range influences the dissipation rate of all the waves coupled. In particular, at a fixed total rms energy, dissipation is reduced if the energy of the higher frequency waves is comparable to the lower frequency ones (flatter spectra) with respect to the case in which most of the energy is contained in the low frequency modes (steeper spectra).

The form of the nonlinear term may be heuristically derived from the following arguments. When eq. (1) is Fourier decomposed ($z^{\pm} \rightarrow z^{\pm}_{\mathbf{k}} = u_{\mathbf{k}} \mp b_{\mathbf{k}}$) nonlinear terms couple several wave numbers in the k-space. When a strong magnetic field (V_a in velocity unit) is present, the propagation time of the Alfvén waves $\tau_a = (\mathbf{k} \cdot \mathbf{V_a})^{-1}$ is equal or longer than the characteristic time-scale for nonlinear interaction $\tau_{NL} = (kv_k)^{-1} \approx (kb_k)^{-1}$, the nature of the nonlinear cascade is highly anisotropic, developing preferentially in planes perpendicular to the direction of the mean field. It is than useful to decompose local wavenumber in projections along the magnetic field ($\mathbf{k}_{||}$) and in the perpendicular planes ($\mathbf{k}_{\perp}$) because energy transfer occurs only among the latter, so that Fourier decomposition is exploited only in $\mathbf{k}_{\perp}$. When small fluctuation are considered $V_a \gg b_k \approx v_k$ these arguments lead to the so called RMHD description which can be derived as an expansion of the usual MHD equation in the small parameter $\epsilon_{RMHD} = \tau_{NL}/\tau_a$ (see Oughton et al., 2004 and reference therein for more details on RMHD), in which variation along the perpendicular directions are decoupled from those along the magnetic field ($\boldsymbol{\nabla} = \boldsymbol{\nabla}_{\perp} + \boldsymbol{\nabla}_{||}$, with $\boldsymbol{\nabla}_{\perp} \gg \boldsymbol{\nabla}_{||}$).

We can describe the global effect of this perpendicular cascade by means of two quantities at the large scales, namely an integral scale λ_0, giving the dimension of the greatest eddies in which energy is injected, and the average velocities difference (Δv) among points belonging to the same eddy, which in RMHD turbulence also contains magnetic field fluctuations in velocity units ($\Delta b/\sqrt{4\pi\rho}$). Identifying these two quantities with the integral turbulent length ($\lambda_0 = L$) and the fluctuations' amplitude of the Elsässer fields we can construct a characteristic timescale $\tau^{\pm}_{NL} = L/|\mathbf{Z}^{\mp}|$ which accounts for nonlinear turbulent interactions in eq.(1).

The nonlinear model equations become, after Fourier transform in time:

$$\frac{d\mathbf{z}^{\pm}}{dr} - i\frac{\omega}{U \pm V_a}\mathbf{z}^{\pm} + \frac{1}{2}\frac{A'}{A}\frac{U \mp V_a}{(U \pm V_a)}\mathbf{z}^{\mp} + \frac{1}{2}\frac{\mathbf{z}^{-} - \mathbf{z}^{+}}{U \pm V_a} \times$$

$$\times \left[\frac{A'}{A}\left(V_a \mp \frac{1}{2}U\right) + \frac{d}{dr}\left(V_a \mp \frac{1}{2}U\right)\right] = -\frac{\mathbf{z}^{\pm}|\mathbf{Z}^{\mp}|}{L(U \pm V_a)} \quad (6)$$

(again L is expressed in units of $R_{\odot}$, and velocities in units of c_s).

The dissipative feature of the nonlinear terms can be shown multiplying eq.6 by the complex conjugate $\mathbf{z}^{\pm *}$ to obtain the evolution equations for the Elsässer energies at a given frequency $E^{\pm} \equiv \frac{1}{2}|\mathbf{z}^{\pm}(\omega)|^2$. It is than evident how nonlinear terms produce a dissipative effect (on the RHS we have the form $-|\mathbf{z}^{\pm}|^{\mathbf{2}}|\mathbf{Z}^{\mp}|/[(U \pm V_a)L]$), which is independent of the phase difference between the two fields and involves the total amplitude of the fluctuations.

2.3 Initial conditions

Eqs.6 are integrated backwards from the Alfvénic critical point till the coronal base. The amplitude of the outgoing wave is imposed while the ingoing wave amplitude is determined demanding the regularity of the solutions at the singularity (the Alfvénic critical point). The spectra are then fixed at the top of the layer and propagated back, the reference value for the power-law scaling is the amplitude of the wave at lowest frequency coupled (fundamental mode), i.e. $z^{+}(\omega_0)$, while the Elsässer energy of the higher frequency waves (interacting mode) scales as $(\omega_i/\omega_0)^{-5/3}$. We fix our attention on the coupling formed with the following frequencies, $\omega_0 = 10^{-6}$, $\omega_1 = 10^{-4}$ and $\omega_2 = 10^{-2}$ for two reasons. The first is that we cover the range in which Alfvénic turbulence is observed at $1\ AU$, the second refers to results coming from linear analysis. When propagation in a non-uniform moving medium is considered total wave action density is conserved (a generalization of total wave energy flux) and with appropriate boundary conditions one can define a transmission coefficient. Actually in the range considered the transmission coefficient shows the highest frequency dependence behavior (see Velli, 1993) causing spectra modifications during wave propagation in absence of nonlinear interactions.
Once nonlinear terms are introduced we loose the predictive feature of the linearized equation for which given an increment of a factor f in the initial conditions we have an equal increment f for the values at the base, hence, to get realistic values of velocity and magnetic field fluctuations at the base of the atmosphere, we have to tune the amplitude of the outgoing wave imposed at the Alfvénic critical point for every frequency and coupling considered. These amplitudes are constrained by measures of line broadening which give root mean squared values approximately between $20\ km/s$ and $30\ km/s$ (Chae et al. , 1998) for coronal temperature.
In the isothermal case the atmosphere parameters are imposed at base of the layer: $\beta_0 = 0.08$ (i.e. $V_{a0} = 5 \times c_s$) for all the temperatures considered which vary between $1 \times 10^6\,K$ and $3 \times 10^6\,K$ (corresponding to $10 \leq \alpha \leq 4$). For the non-isothermal layer we impose $T_0 = 0.8 \times 10^6 K$ and $T_{max} = 3.5 \times 10^6\ K$ at $R_{max} \sim 3R_{\odot}$ ($\beta_0 \sim 0.01$). In both cases the magnetic field at the base is $B_0 \sim 10\,G$ and densities are of the order of $10^8\ cm^{-3}$.

3. RESULTS

To quantify dissipation we look at the linearly conserved quantity, that is total wave action density at the bottom and top boundary (S^*_0 and S^*_c respectively). Dissipation efficiency, $\gamma \equiv (S^*_0 - S^*_c)/S^*_0$, accounts for dissipation in

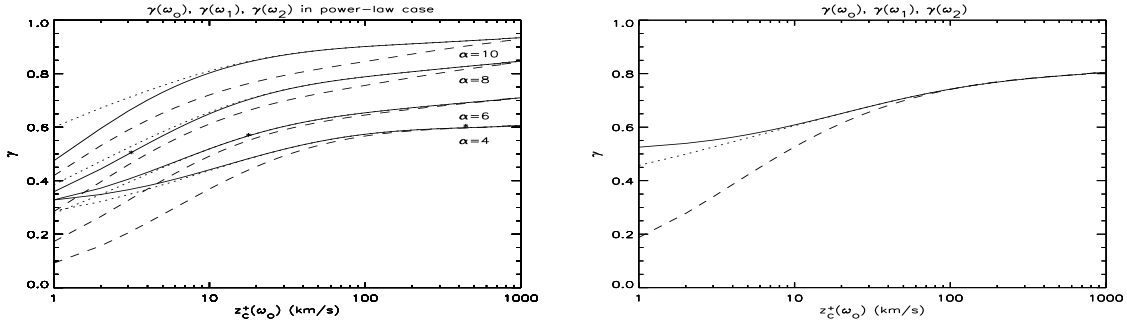

Figure 1. Dissipation efficiency as function of initial outgoing wave amplitude $z_c^+(\omega_0)$ imposed at the top of the layer for an isothermal (left panel) and a non-isothermal layer (right panel). Initial wave amplitude is scaled following a power-law spectrum (see text). The different plots refer to atmospheres with $\alpha = 4, 6, 8, 10$, solid, dotted and dashed line represents respectively $\gamma_{\omega 0}$, $\gamma_{\omega 1}$ and $\gamma_{\omega 2}$.

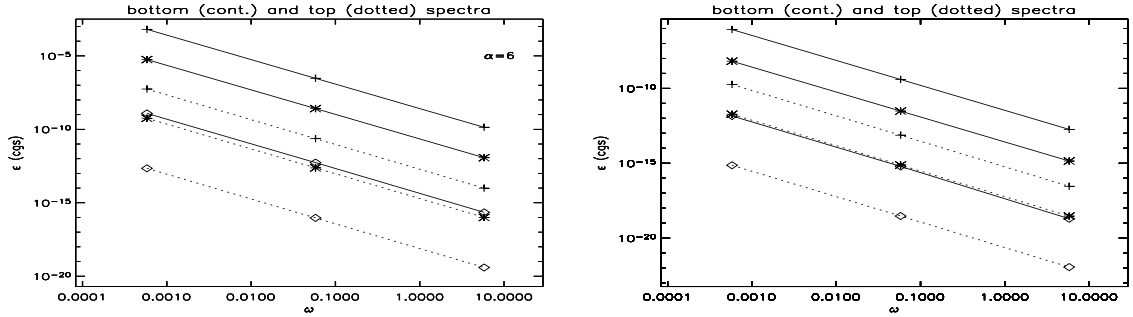

Figure 2. Spectra at the top (dotted line) and the bottom (solid line) of the atmosphere for three representative initial values of $z_c^+(\omega_0)$ ($1\,km/s$, $100\,km/s$ and $1000\,km/s$ marked with crosses, stars and diamonds respectively). Left panel: isothermal layer ($\alpha = 6$). Right panel: non-isothermal layer

the whole layer. In fig.1 dissipation efficiency is plotted as function of the fundamental mode initial wave amplitude for a power-law initial spectrum in both isothermal (various temperature) and non-isothermal layer (left and right panel respectively); solid, dotted and dashed lines refers respectively to $\gamma_{\omega 0}$, $\gamma_{\omega 1}$ and $\gamma_{\omega 2}$. For both kinds of atmospheres the three curves relative to the coupled waves show that for intermediate frequency (dotted line) dissipation efficiency soon reaches the fundamental mode regime even in the coolest atmospheres, while for the high frequency interacting waves (dashed line) this condition is achieved for higher initial amplitudes (roughly greater than $50\,km/s$). A major difference between cool and hot atmospheres is the behavior of the intermediate frequency which, for low enough initial amplitude shows a more efficient dissipation than the fundamental mode. For cooler atmospheres and weak couplings (low wave amplitudes) the wind carries low frequency waves out to the Alfvénic critical point reducing their reflection. So one can actually separate very low frequency behavior (wave mainly transmitted, poor dissipation) from intermediate frequency behavior (wave mainly reflected and strong dissipation) only for small enough waves amplitudes.

Differences between the two kind of atmospheres originate mainly from the different expansion rate. A higher stratification produces a stronger reflection and one should expect an enhanced dissipation efficiency for all the amplitudes considered. If we compare the results with the hotter atmospheres ($\alpha = 4,\ 6$) we see that it is actually true. Temperature variation mainly modifies the wind solution. As in the $\alpha = 4$ atmosphere, which has approximately the same temperature of the peak of the non isothermal layer, the wind is not able to greatly reduce the amount of reflection for the low frequency - low amplitude waves. This is also due to the fact that the β of the plasma is very low and Alfvén wave gradients are mainly responsible of wave reflection. In the linear case, a so strong Alfvén speed produces a shift toward higher values of the critical frequency, defined as the frequency beyond which waves are completely transmitted. Hence reflection (and dissipation) at high frequencies is enhanced. The result is that despite strong reflection we don't find an enhanced frequency dependence, dissipation efficiency of the three coupled waves reach again the same value approximately for the same wave amplitude of the non-expanding case. To guess the modifications of initial spectra (top of the layer) one can look at dissipation efficiency. If in fact it is the same for all the coupled frequencies (strong coupling) we expect the spectrum to remain almost unchanged during wave propagation.

In fig.2 the spectra $\epsilon = \rho(|z^+(\omega_n)|^2 + |z^-(\omega_n)|^2)$ im-

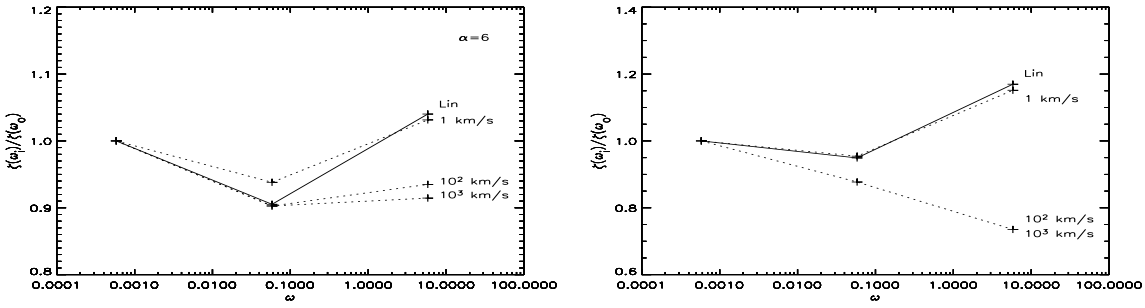

Figure 3. Normalized ratio ξ (dotted lines) for the two cases in fig.2: values lower -greater- than one mean spectrum is steepening -flattering- (see text for details). For comparison the linear case is also shown (continuos line).

posed at the top of the atmosphere (dotted line) and those at the base of the atmosphere (solid line) are plotted for two different layers, isothermal ($\alpha = 6$) and non-isothermal (respectively on the left and right panel). Three representative initial wave amplitudes for the fundamental frequency are considered, $z_c^+(\omega_0) = 1,\ 100,\ 1000\ km/s$ and frequencies are marked with different symbols (crosses, stars and diamonds) to distinguish the three initial amplitudes. Since we impose a power-law spectrum at the top of the layer all dotted lines have slope $-5/3$ and can be used as reference to see the modification induced by wave propagation. It is striking how much the spectra remain unchanged practically for all temperatures and all initial amplitudes considered. The different energy contained in the spectra is mainly due to difference in mass density at the critical point which for the non isothermal case is located at $\sim\ 12\ R_\odot$ and for the isothermal atmosphere ($\alpha = 6$) at $\sim\ 6\ R_\odot$. A more accurate inspection, using the ratio $\xi(\omega_i) = \epsilon_c(\omega_i)/\epsilon_0(\omega_i)$ shows that the spectra do change slightly. In fig.3 we plot such ratios normalized to the value of the previous frequency, i.e. $\xi(\omega_1)/\xi(\omega_0)$ and $\xi(\omega_2)/\xi(\omega_1)$ (the fundamental being normalized to its value). Since the top spectrum is fixed by the initial condition a normalized value lower (greater) than one means the spectrum is steepening (flattening) with respect its shape at the atmospheric base. Consider first the isothermal layer (left panel). For low initial amplitudes the coupling is not strong and the spectrum evolution is similar to the linear case, it steepens at low frequencies and flattens at the higher ones. As we increase the strength of the coupling by increasing $z_c^+(\omega_0)$, at low frequencies the spectrum steepens (reaching the linear value). At higher frequencies it steepens too, asymptotically reaching the same slope of the low frequency part (the effect of a strong coupling).

Consider now the non-isothermal supra-spherical expanding wind (right panel), for which a different scale as been adopted. Here modifications to the spectra are more evident. For low initial amplitudes the spectrum steepens at low frequencies and flattens at higher frequencies, approximately the same way as in the linear case. As we increase the energy contained in the fundamental mode the spectrum globally steepens, being unchanged for amplitudes greater than $100\ km/s$ and most steep for high frequencies waves. To quantify spectral evolution we have calculated the exponent of the resulting power-law scaling at the base for the low and high frequency branches. For the isothermal case the slope at the base varies from 1.644 at low frequencies to 1.673 at higher frequencies, to be compared with 1.66667 (top spectrum). One can conclude that even if the spectra evolves during propagation the differences between top and bottom slopes are always very small or negligible. For the non-isothermal layer the slopes varies from 1.598 to 1.701 indicating a somewhat greater evolution of the spectra.

4. CONCLUSIONS

In this paper we have modeled the nonlinear evolution of Alfvén waves propagating through the subalfvénic region of stellar winds. Nonlinear interactions occur between outward propagating and reflected waves, and it is assumed that a nonlinear cascade develops preferentially in a direction perpendicular to that of propagation. The nonlinear term acts as a dissipative sink for both outward and inward waves of a given frequency. The stratified atmosphere is in spherical or supra-spherical expansion and the plasma parameter ($\beta = 8\pi P/B^2$) at the base of the layer, identified with the coronal base, has been kept fixed for the isothermal case. Equations are integrated out to the Alfvénic critical point (wind speed equal to the Alfvén speed) whose location moves to greater distances from the base as temperature is decreased (for the non-isothermal layer it is placed at about $12\ R_\odot$).
With regard to the amount of dissipation generally we can say that the lower the temperature of the layer, and the lower the frequency of the coupled waves, the higher the dissipation. However in this paper we focused our attention on modification of a sample spectrum with three rappresentative frequencies $10^{-6}\,Hz$, $10^{-4}\,Hz$ and $10^{-2}\,Hz$.

As mentioned in paragraph 2.3 nonlinearities break the scaling properties at the boundaries typical of a linearised equation. We used solar observational constraints to define the amplitudes to impose at the top boundary, depending on the kind of atmosphere considered and on

temperatures. For an $\alpha = 6$ isothermal layer corresponding to a temperature of $2 \times 10^6 K$ (roughly the solar case), we find amplitudes for the fundamental mode in the range of $79\,km/s$ and $117\,km/s$. For these amplitudes the coupling is strong and spectra don't evolve appreciably. For the non-isothermal supra-spherical expanding wind we find higher values, i.e. $164\ km/s$ and $236\ km/s$ lying in the range in which the spectrum globally steepens.
Generally we can say that when a non local strong coupling is considered (high amplitudes), nonlinear terms smooth differences in the dissipation of waves of different frequencies (caused by the different reflection). For low energies in the fundamental mode, waves evolves almost independently and the dissipation rate of a given frequency wave can be guessed by its transmission coefficient (linear analisys).

There are other aspects which may modify the results presented here. For instance, we have adopted a constant dissipative turbulent length scale and nonlinear terms in eq.6 become dominant in the outer region (the other gradients reduces, this one remains constant) hence enforcing the coupling. An expanding (spherically or supraspherically) turbulent length scale reduces greatly the effects of nonlinearities making the spectra evolution more similar to the linear one.

In order to get a complete answer to the question of turbulent evolution the actual nonlinear cascade must be taken into account as well as propagation. Despite more work has still to be done, one can preliminarily conclude that turbulence is not able to produce substantial modification of the original spectrum atmosphere, starting from the coronal base, at least until the Alfvénic critical point. Beyond this limit the evolution of turbulence is decoupled from the source from which it originates since all the waves (propagating outward or inward) are advected by the wind at a speed much greater than the Alfvén speed. For the solar case an interesting development is the extension of this analysis to deeper layer in the atmosphere, where flux tube expansion and gradients are so strong as to produce, in the linear regime, a very strong frequency dependent transmission. This might produce significant changes in spectral properties with height.
This research was partially funded by EU Contract n. HPRN-CT-2001-00310 and MIUR PRIN (COFIN) contract 2002025872.

REFERENCES

Hollweg J. V., Bird M. K., Volland H., Edenhofer P., Stelzried C. T. and Seidel B. L., *J. Geophys. Res.*, **87**, 1-8, 1982

Scott S. L., Coles W. A. and Bourgois G., *Astron. Astrophys.*, **123**, 207-215, 1983

Velli M., *Astron. Astrophys.*, **270**, 304-314, 1993

Velli M., Grappin R. and Mangeney A., *Geophys. Astrophys. Fluid Dyn.*, **62**, 101, 1991

Chae, J., Yun HS and Poland, ApJ 480, 817, 1998

Mangeney A.,Grappin R. and Velli M., in Priest E. R., Hood A. W. (eds.) *Advances in Solar System Magnetohydrodynamics*, p.327, 1991

Lou Y. Q. and Rosner R., *Apj*, **424**, 429-435, 1994

Krogulec M. and Musielak Z. E., *ACTA ASTRON.*, **48**, 77-90, 1998

Krogulec M., Musielak Z. E., Suess S. T., Nerney S. and Moore R. L., *J. Geophys. Res.*, **99A**, 23489, 1994

Heinemann M. and Olbert S., *J. Geophys. Res.*, **85A**, 1411, 1980

Leroy B., *Astron. Astrophys.*, **91**, 136, 1980

Leroy B., *Astron. Astrophys.*, **97**, 245, 1981

Moore R. L., Musielak Z. E., Suess S. T. and An C. H., *Astrophys. J.*, **378**, 347, 1991

Similon P. L. and Zargham S., *Astrophys. J.*, **388**, 644, 1992

Dmitruk P., Matthaeus W. H., Milano L. J. and Oughton S., *Bull. Am. Phys. Soc.*, **45**, 187, 2000

Dmitruk P., Milano L. J. and Matthaeus W. H., *Astrophys. J.*, **548**, 482-491, 2001

Dmitruk P., Matthaeus W. H., Milano L. J., Oughton S., Zank G. P. and Mullan D. J., *Astrophys. J.*, **575**, 571-577, 2002

Dmitruk P. and Matthaeus W. H., *Astrophys. J.*, **597**, 1097-1105, 2003

Oughton S., Matthaeus W. H., Dmitruk P., Milano L. J., Zank G. P. and Mullan D. J., *Astrophys. J.*, **551**, 565-575, 2001

Oughton S., Dmitruk P. and Matthaeus W. H., *Physics of Plasmas*, **Vol. 11, N. 5**, 2214, 2004

Kopp R. A. and Holzer T. E., *Sol. Phys*, **49**, 43, 1976

Munro R. H. & Jackson B. V., *Astrophys. J*, **213**, 874, 1977

Casalbuoni S., Del Zanna L., Habbal S. R. and Velli M., *J. Geophys. Res.*, **104**, 9947-9961, 1999

Verdini A, Velli M. and Oughton S., *Astron. Astrophys*, submitted